DESIGN AND PERFORMANCE SIMULATION OF A HIGH SPEED BRUSHLESS DC MOTOR FOR EMBROIDERY MACHINE APPLICATION

Chen Jiaxin*, Guo Youguang†, Zhu Jianguo†

*College of Electromechanical Engineering, Donghua University, China. Email: chjiaxin@dhu.edu.cn
†Faculty of Engineering, University of Technology, Sydney, Australia. Email: youguang@eng.uts.edu.au, joe@eng.uts.edu.au

Keywords: High speed motor, brushless DC motor, magnetic field finite element analysis, incremental inductance, performance simulation.

Abstract

This paper presents an improved phase variable model and field-circuit coupling method for the design and performance analysis of a high speed surface mounted permanent magnet brushless DC motor. In the design of the motor, magnetic field finite element analysis is conducted to calculate the key motor parameters such as the air gap flux, back electromotive force, and inductance, etc. Based on the numerical magnetic field solutions, a modified incremental energy method is employed to effectively calculate the self and mutual inductances of the stator windings. An equivalent electrical circuit is derived to predict the motor characteristics. In order to study the comprehensive performance of the motor at the design stage, especially the motor output speed and torque at high speeds, which are affected by the dynamic inductances, an improved phase variable model is introduced to simulate the motor performance. The motor prototype has been constructed and tested with both a dynamometer and a high speed embroidery machine, which validates successfully the theoretical calculations.

1 Introduction

High speed permanent magnet (PM) motors with brushless DC control scheme have found wide applications in industrial and domestic appliance drive market because of their advantages such as high efficiency, high power density and high drive performance [1]. This paper presents the development of a PM brushless DC motor for driving high speed embroidery machines. In the design of the motor, the magnetic field finite element analysis (FEA) is conducted to calculate the key motor parameters such as the air gap flux, back electromotive force (*emf*), and inductance, etc. Based on the numerical magnetic field analysis, a modified incremental energy method is applied to effectively calculate the self and mutual inductances of the stator windings. An equivalent electric circuit is derived to predict the motor performance. The rise rate of armature current is limited by the winding inductances, and this may affect the output performance of the motor, especially when operating at high speed. Therefore, it is necessary to investigate whether or not the motor can reach the required electromagnetic torque and speed at a given voltage. An improved phase variable model based on Simulink is developed [3], and by using this model, the performance of motor is predicted.

2 Motor configuration and major dimensions

Fig. 1 illustrates the magnetically relevant parts of the motor prototype. The laminated stator has 12 slots, in which the three phase single-layer windings are placed. The rotor core and shaft are made of solid mild steel, and four pieces of NdFeB PMs are mounted and bound on the surface of the rotor. The stator core has an inner diameter of 38 mm, outer diameter of 76 mm, and axial length of 38 mm. The main air gap length and the height of PMs along the radial magnetization direction are chosen as 1 mm and 2.5 mm, respectively. The motor is designed to deliver an output torque of 1.0 Nm at a speed of not less than 5000 rev/min under the rated voltage of 310 V.

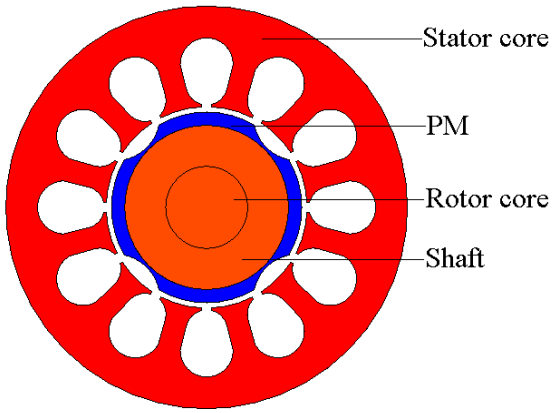

Fig. 1: cross section of the PM brushless DC motor.

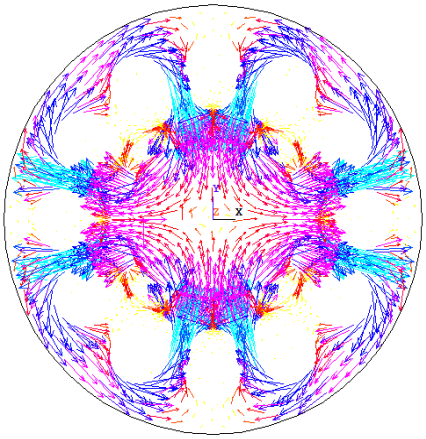

Fig. 2: plot of no-load magnetic flux density vectors.

3 Computation of motor parameters and performance

3.1 Winding flux, back *emf* and cogging torque

Magnetic field FEA can take into account the detailed structure and dimensions of the motor and the non-linearity of ferromagnetic materials, and hence can accurately compute the motor parameters and performance. Fig. 2 illustrates the magnetic field distribution at no-load at the rotor position shown in Fig. 1, from which the phase winding flux produced by the rotor PMs, back *emf*, and cogging torque can be determined. The curves of these parameters against the rotor angular position or time can be obtained by a series of magnetic field FEAs at different rotor positions. Fig. 3 shows the no-load flux linking a coil (two coils form a phase winding) at different rotor positions. By the discrete Fourier transform, the magnitude of the fundamental of the coil flux is calculated as ϕ_1=0.543 mWb, and the *emf* constant can then be determined as 0.2457 Vs/rad, by

$$K_E = \frac{p}{2} N_s \frac{\phi_1}{\sqrt{2}} \tag{1}$$

where p=4 is the number of poles and N_s=320 is the number of turns of a phase winding. The electromagnetic torque constant can be obtained by $K_T = mK_E$, where m=3 is the number of phases.

From the no-load magnetic field distribution, the cogging torque curve can also be calculated by the Maxwell stress tensor method, or the virtual work method. It was found that the cogging torque of this surface-mounted PM motor is very small with a maximum value of 0.014 Nm.

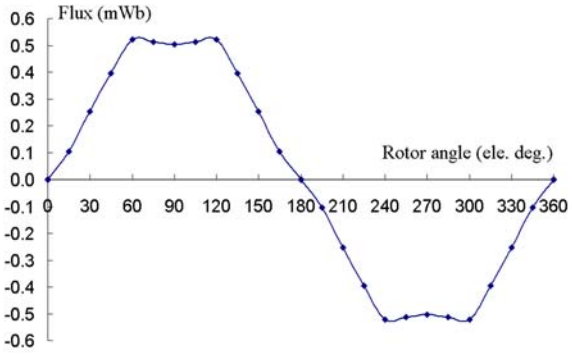

Fig. 3: flux linking a coil versus rotor angle at no-load.

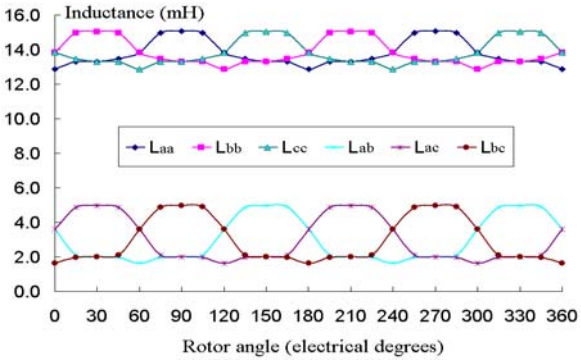

Fig. 4: winding inductances versus rotor angle.

3.2 Winding inductance

The behavior of the motor equivalent electrical circuit is determined by the incremental inductances instead of the apparent ones [4]. In this paper, the winding incremental inductances are calculated by a modified incremental energy method [5], which includes the following steps: (1) For a given rotor position θ, conduct a non-linear field analysis considering the saturation due to the PMs to find the operating point of the motor, and save the incremental permeability in each element; (2) Set the remanence of PMs to be zero, and conduct linear field analyses with the saved permeabilities under perturbed stator current excitations, i.e. assigning the 3 phase winding currents as $(i_a,i_b,i_c) = (\Delta i,\Delta i,0)$, $(\Delta i,0,\Delta i)$, $(0,\Delta i,\Delta i)$, $(\Delta i,0,0)$, $(0,0,\Delta i)$, and $(0,\Delta i,0)$, respectively; (3) Calculate the magnetic co-energy for each current excitation; and (4) Calculate the incremental inductances by

$$L_{aa}(\theta) = L_{bb}(\theta) = L_{cc}(\theta) = \frac{2W_c(\Delta i,0,0,\theta)}{(\Delta i)^2} \tag{2a}$$

$$L_{ab}(\theta) = L_{ba}(\theta) = \frac{W_c(\Delta i,\Delta i,0,\theta) - W_c(0,\Delta i,0,\theta) - W_c(\Delta i,0,0,\theta)}{(\Delta i)^2} \tag{2b}$$

$$L_{bc}(\theta) = L_{cb}(\theta) = \frac{W_c(0,\Delta i,\Delta i,\theta) - W_c(0,\Delta i,0,\theta) - W_c(0,0,\Delta i,\theta)}{(\Delta i)^2} \tag{2c}$$

$$L_{ca}(\theta) = L_{ac}(\theta) = \frac{W_c(\Delta i,0,\Delta i,\theta) - W_c(0,0,\Delta i,\theta) - W_c(\Delta i,0,0,\theta)}{(\Delta i)^2} \tag{2d}$$

Fig. 4 shows the calculated self and mutual incremental inductances at different rotor positions.

3.3 Performance calculation

To predict the motor performance, an equivalent electrical circuit is derived as shown in Fig. 6, where E_1 is the back *emf*, R_1 the stator winding resistance, L_1 the synchronous inductance which equals the self inductance plus half of the mutual inductance, V_1 the rms value of the stator phase voltage, I_1 the phase current, and ω the angular frequency. The motor is assumed to operate in the optimum brushless DC mode, i.e. I_1 in phase with E_1, so that the electromagnetic torque can be obtained by

$$T_{em} = \frac{3E_1 I_1}{\omega_r} \tag{3}$$

where ω_r is the rotor speed in mechanical rad/s. The rms value of the back *emf* is determined by $E_1=k_E\omega_r$. For a given terminal voltage, V_1, the relationship between the rotor speed and electromagnetic torque can be derived as

$$(K_E\omega_r + \frac{R_1 T_{em}}{K_T})^2 + (\frac{p\omega_r L_1 T_{em}}{2K_T})^2 = V_1^2 \tag{4}$$

Fig. 5 illustrates the torque/speed curves with different values of terminal voltage.

4 Equation-based phase variable model

In Section 3, the motor performance was predicted based on sinusoidal waveforms (i.e. the fundamental component) of winding flux, back *emf*, and current. In this section, the motor performance is also studied with the square waveform voltages and the trapezoidal waveform *emfs* by a Matlab/Simulink-based simulation model. This study aims to investigate whether or not the motor can reach the specified speed with the rated load at a given voltage. The motor output can be limited by the effect of the winding inductance, especially at high speed operation.

The equation-based phase variable model of BLDC motor is given as:

$$V_{abc} = r_{abc} i_{abc} + \frac{d\psi_{abc}}{dt} + e_{abc} \tag{5}$$

$$\psi_{abc} = L_{abc} i_{abc} \tag{6}$$

$$T_m = \frac{e_a i_a + e_b i_b + e_c i_c}{\omega_r} + T_{cog} \tag{7}$$

$$J\frac{d\omega_r}{dt} = T_m - B\omega_r - T_L \tag{8}$$

$$L_{ab} = L_{ba}, L_{bc} = L_{cb}, L_{ca} = L_{ac}, r_a = r_b = r_c \tag{9}$$

$$i_a + i_b + i_c = 0 \tag{10}$$

All above variables are used as their conventional meanings. The profiles of L_{abc}, e_{abc}, and T_{cog} are obtained from the nonlinear transient FE solutions, in which the rotor position dependence and the saturation effect are considered.

5 Simulink model and validation

5.1 Simulink implementation

For dynamic performance evaluation, compared with an equivalent electric circuit model, the time-stepping nonlinear FEA procedure can give accurate results but is time consuming. A phase variable model of BLDC motor based on FEA and coupled with external circuits, which behaves much faster with the same level of accuracy, has been introduced and verified in [2]. In this model, the inductances, back *emf* and cogging torque were obtained by nonlinear FEAs, and the problem that the equation-based model cannot be applied to BLDC directly was solved by a method of using a model composed of several circuit components indirectly. Another method of pure mathematic method was proposed [3]. By using this method, the voltage of central point of the Y-type three phase windings can be obtained, and the equation-based model of BLDC motor can be applied to the BLDC simulation system directly. The details have been introduced in [3], so in this paper only the completed phase variable model in Simulink surrounding is given as shown in Fig.7.

5.2 Performance evaluation

The basic design requirement for the motor drive system is that for an output torque of 1.0 Nm, the steady-state speed should be no less than 5000 rpm when the inverter DC bus voltage is V_{dc}=310 VDC. By using the proposed model, the motor drive system is simulated under these conditions and some of the results are plotted in Figs. 8-11, showing that the motor can meet the design requirements.

5.3 Experimental validation

The designed motor has been fabricated and successfully operated with a brushless DC control scheme. Experiments have been conducted on the prototype. The back *emf*, for example, was measured at different rotor speeds and the experimentally determined *emf* constant is 0.2464 Vs/rad, which is very close to the theoretical calculation. Other parameters, such as the inductances and torque/speed curves are also in substantially agreement with the computations.

6 Conclusion

This paper reports the design and analysis of a high speed permanent magnet brushless dc for driving embroidery machines. The motor performance is investigated by an improved phase variable model, which is implemented in Simulink surrounding. For accurate computation of the motor parameters, the finite element magnetic field analysis is performed and improved formulations, e.g. the modified incremental energy method for calculating the self and mutual winding inductances, are used. The motor has been constructed and tested with a brushless DC control scheme, validating the theoretical design and analysis.

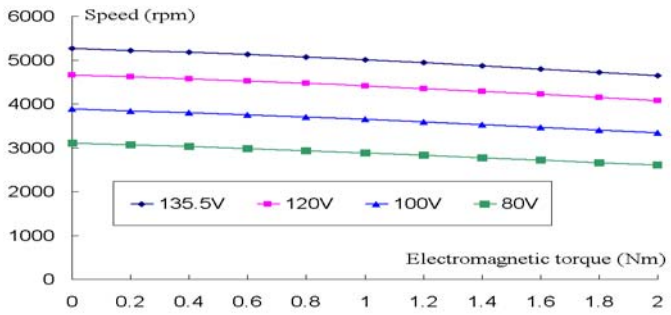

Fig. 5: torque/speed curves at different phase voltages.

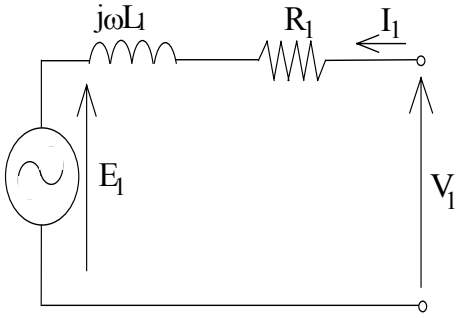

Fig. 6: per-phase equivalent electrical circuit.

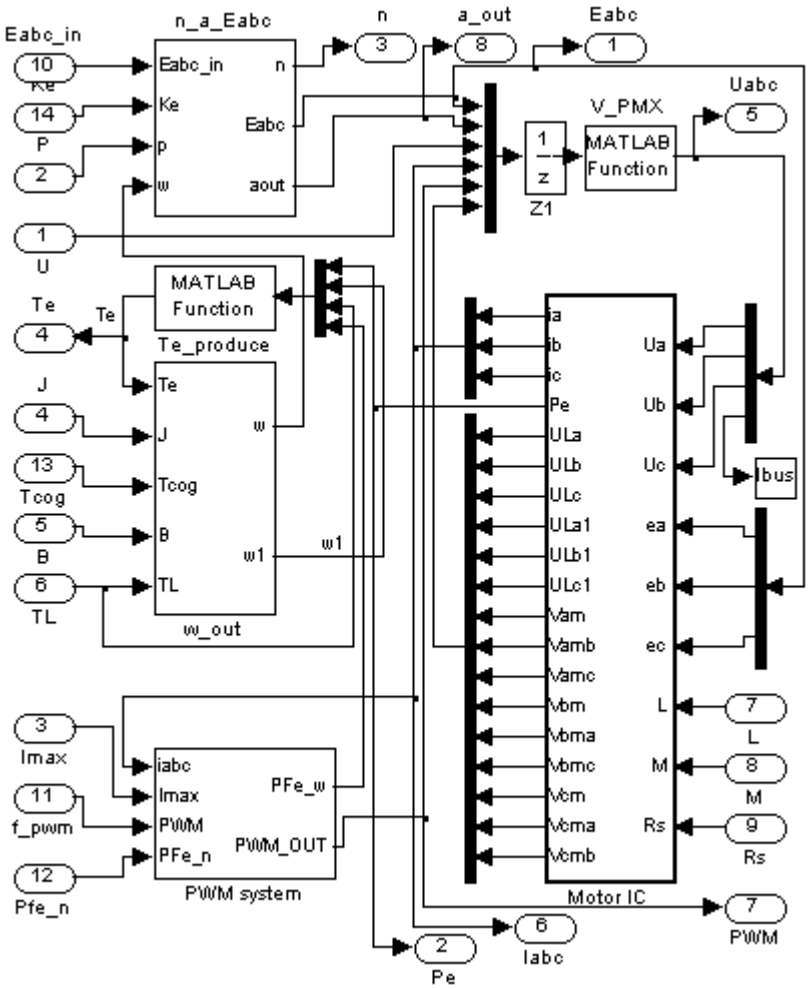

Fig. 7: diagram of the phase variable model.

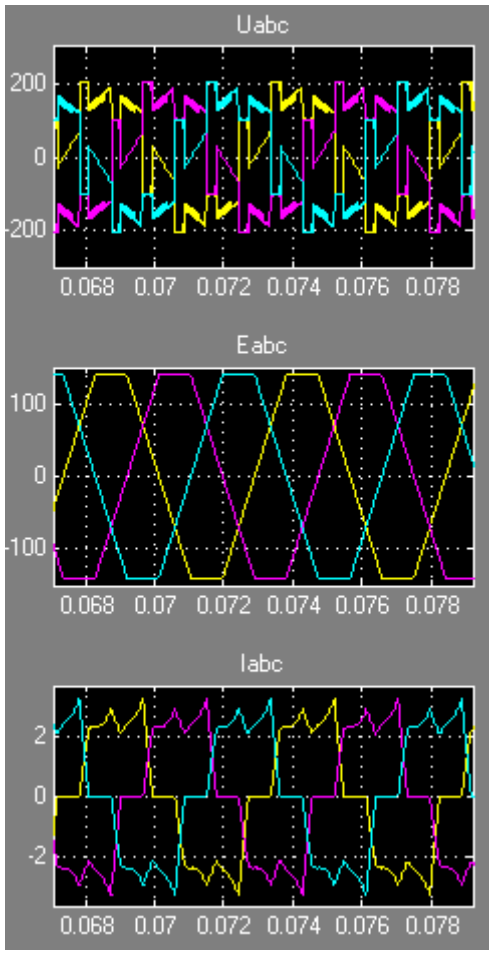

Fig. 8: steady performance at T_L=1.0 Nm and VDC=310 V (X-axis: Time in s).

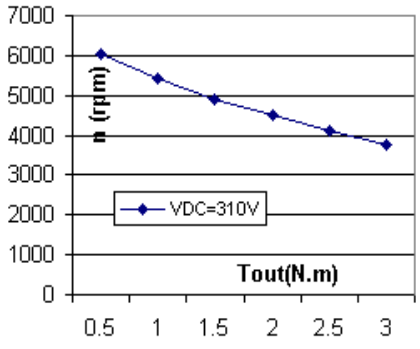

Fig. 9: torque vs speed curve.

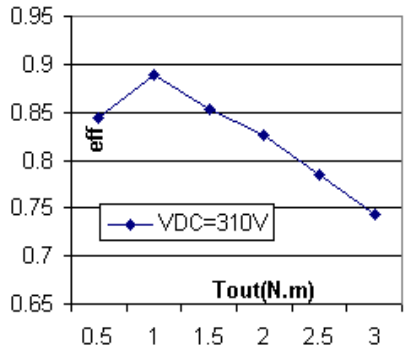

Fig. 10: torque vs efficiency curve.

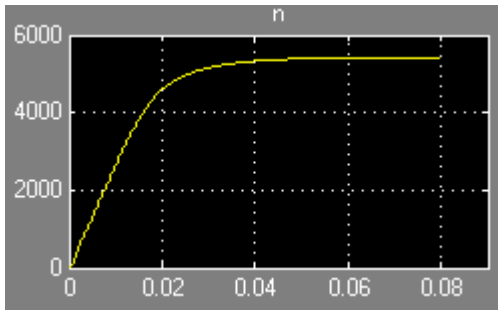

Fig. 11: start-up performance with T_L=1.0 Nm and VDC=310V (X-axis: Time in s).

References

[1] T. Kenjo, "Permanent Magnet and Brushless DC Motors", *Oxford University Press*, 1985.

[2] O.A. Mohammed, S. Liu, Z. Liu, "A phase variable model of brushless dc motors based on finite element analysis and its coupling with external circuits," *IEEE Trans. Magn.*, **41**, 1576-1579, 2005.

[3] Jiaxin Chen, Youguang Guo, Jianguo Zhu, "Comprehensive performance evaluation of permanent magnet brushless dc motor in dynamic condition by a phase variable model," presented to *Asia-Pacific Symposium on Applied Electromagnetics and Mechanics*, Sydney, Australia, July 20-21, 2006.

[4] M. Gyimesi, D. Ostergaard, "Inductance computation by incremental finite element analysis," *IEEE Trans. Magn.*, **35**, 1119-1122, 1999.

[5] Y.G. Guo, J.G. Zhu, H.Y. Lu, "Accurate determination of parameters of a claw pole motor with SMC stator core by finite element magnetic field analysis," *IEE Proceedings – Electric Power Application,* **153**(4): 568-574, 2006.